A Comprehensive Analysis of Packet Delay in Reconfigurable Intelligent Surface-Assisted Communication Networks

Ahmed I. Abdulshakoor[1], Najah Abu Ali[2], Hossam S. Hassanein[3]
[1]*Department of Electrical and Computer Engineering, Queen's University, Kingston, ON, Canada*
[2]*College of Information Technology, United Arab Emirates University, Al-Ain, UAE*
[3]*School of Computing, Queen's University, Kingston, ON, Canada*
Emails: 21aia1@queensu.ca, najah@uaeu.ac.ae, hossam@cs.queensu.ca

ICC 2024 - IEEE International Conference on Communications | 978-1-7281-9054-9/24/$31.00 ©2024 IEEE | DOI: 10.1109/ICC51166.2024.10622665

***Abstract*—Reconfigurable intelligent surface (RIS) technology has been widely used to enhance the performance of wireless communication networks. Specifically, to overcome the blockage issue, the RIS is equipped with passive elements that can steer the wireless signals around the obstacle and construct a virtual line-of-site (LoS) link between the transmitter and receiver. This paper presents a comprehensive analysis of packet delay in RIS-assisted communications, an area that has received limited attention in the literature. Our analysis carefully examines the cascaded wireless channel via RIS to calculate the signal-to-noise ratio (SNR) distribution within Nakagami-m fading channels. Furthermore, we utilize the SNR distribution to develop a novel expression for average packet delay. Our method was evaluated thoroughly through numerical and simulation-based performance testing. We explored the impact of various parameters on average delay performance, including the number of reflecting elements, average SNR, and distance between the user and RIS. Our research indicates that a larger number of passive reflecting elements in an RIS can significantly improve signal reception at the user, leading to better average packet delays. The findings of this paper can be used in multi-user scenarios, where the packet delay is one of the metrics used to address the user-RIS association problem based on the user's delay requirements.**

***Index Terms*—Reconfigurable Intelligent Surface (RIS), Nakagami-m channels, 5G and NextG networks, Average packet delay.**

I. Introduction

Reconfigurable intelligent surface (RIS) technology has received significant attention due to its ability to enhance the performance of wireless communication networks. A RIS consists of numerous low-cost passive reflecting elements that can be configured to shape and redirect the wavefront of a radio signal and create a controllable wireless channel [1]. From an energy standpoint, RISs are very efficient; they can reshape and forward the radio signals impinging on them without a power supply, radio frequency (RF) chains, or complicated signal processing techniques. Therefore, to enhance network coverage, RISs can be densely distributed within the network's infrastructure at a lower cost and without complicated management, consequently, promising wide improvement in the quality and reliability of wireless communication services. This opens up numerous promising applications for future wireless networks integrated with an RIS scheme. Since physical obstructions constitute a significant problem for signal propagation and degrade the connectivity; RIS can be used to expand and enhance the network coverage. Specifically, to overcome blockage issue, the RIS is equipped with passive elements that can steer the wireless signals around the obstacle and construct a virtual line-of-site (LoS) link between the transmitter and receiver. Therefore, due to its ability to enhance network coverage and capacity by tuning the wireless propagation in a smart and passive manner, RIS is receiving a great deal of attention.

A method for measuring cellular network performance is analyzing the average packet delay, which is the required time for a data packet to be delivered from its source to its intended destination. Such delay can significantly impact the overall system performance, especially for real-time applications. Therefore, analyzing the average packet delay in cellular networks identifies performance issues. Furthermore, by analyzing packet delay, network operators can allocate network resources, schedule users' traffic more efficiently, and ultimately provide customers with better quality of service (QoS).

The performance of RIS-assisted wireless systems has been investigated in several works [2]–[11]. The authors in [2] studied the performance of the RIS-assisted networks by analyzing the outage performance and error rate, as well as the channel capacity of the network. In [3] and [4], the efficiency and coverage of different RIS-assisted systems are investigated in terms of network capacity, outage probability, and the symbol error rate of the systems. The authors in [5] and [6], presented the performance of wireless communication systems integrated with RIS by deriving the outage probability, average bit error rate (BER), and average capacity of the considered systems. In [7], a mathematical framework is proposed to evaluate the performance of a RIS-enabled network. They presented a performance analysis and investigated the effect of different parameters, including the outage probability and average BER. In [8], the RIS enhances link security from the access point to legal devices. They evaluated the secure

Authorized licensed use limited to: Queen's University. Downloaded on August 21,2024 at 11:21:21 UTC from IEEE Xplore. Restrictions apply.

performance of devices using average secrecy rate and secure outage probability metrics. Although RIS-assisted networks have been studied in various wireless schemes [9]–[11], most existing works use standard metrics to evaluate the system's performance. These metrics include outage probability, ergodic capacity, BER, and energy efficiency. Recently, authors of [12] introduced a new metric called effective energy efficiency, which relies on effective capacity and network power consumption. They addressed delay-outage probability for QoS guarantee, with this probability being influenced by the QoS exponent parameter. A higher QoS exponent value implies more stringent delay-QoS constraints. The authors developed an optimization framework for effective energy efficiency based on the chosen QoS exponent value, which represents the delay requirements of users.

The advent of 5G and NextG networks has made it crucial to ensure smooth communication with minimal delay. Although RIS holds great promise in enhancing network performance, we remark that the current research on RIS-assisted networks mainly focuses on the aforementioned metrics. Hence, there is still a gap in understanding the RIS impact on packet delay, a critical parameter for real-time applications and overall network efficiency. To the best of our knowledge, our work is the first to consider packet delay analysis over RIS-assisted links. Our contributions are outlined as follows:

- Our research provides a comprehensive analysis of the signal-to-noise ratio (SNR) distribution over cascaded Nakagami-m fading wireless channels between a source and destination via RIS reflections.
- We used this analysis to develop a closed-form expression to calculate the average packet delay, which fills a significant knowledge gap in the field.

A thorough evaluation of our method is conducted through numerical and simulation-based performance evaluation, exploring the effects of various RIS-specific parameters, such as the number of passive reflecting elements on packet delay.

The rest of this paper is organized as follows. In section II, the system model is described. Section III provides a detailed analysis of the average packet delay over RIS-assisted links. The performance evaluation and simulation results are provided in section IV, and finally, Section V concludes this paper.

II. System Model

Consider a downlink communication system that employs RIS technology as illustrated in Fig.1. This system consists of a transmitting base station (BS), user equipment (UE) as a receiver, and a RIS deployed between them. Let $\mathbf{h} \triangleq [h_1, h_2, ..., h_N]^T \in \mathbb{C}^{N\times 1}$, and $\mathbf{g} \triangleq [g_1, g_2, ..., g_N]^T \in \mathbb{C}^{N\times 1}$, represent the baseband equivalent channels between the BS and RIS, and from the RIS to the UE, respectively. We assume that the direct link from the BS to UE cannot be formed due to blockage, then the RIS can provide an intelligent environment to improve the signal quality while satisfying the user's requirements. The BS and user are equipped with one antenna, and the RIS comprises N passive reflecting elements.

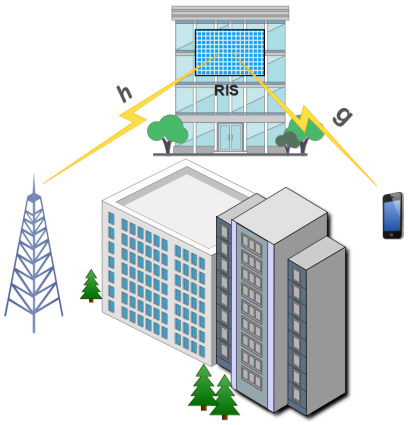

Fig. 1. Reconfigurable Intelligent Surface-assisted wireless system.

It is assumed that the RIS has the capability to acquire the channel state information (CSI) of the constructed channels. This information helps to determine the optimal phase shifts that maximize the SNR received by the UE. The paper assumes a quasi-static flat-fading channel model, where all channels stay nearly constant throughout each coherence interval for the channel.

Let $\theta \triangleq [\theta_{\mathbf{1}}, \theta_{\mathbf{2}}, ..., \theta_{\mathbf{N}}]^{\mathbf{T}} = [\eta_1 e^{j\phi_1}, \eta_2 e^{j\phi_2}, ..., \eta_N e^{j\phi_N}]$ represent the equivalent reflection coefficients of the RIS, where $\eta_n \in [0, 1]$ and $\phi_n \in [0, 2\pi)$, $\forall n = [1, 2, ..., N]$, are the reflection amplitude of element n at the RIS and the corresponding phase shift, respectively. The reflection amplitude of each element is configured to its highest value to maximize the RIS signal reflection power, i.e., $\eta_n = 1, n = 1, 2, ..., N$. Then, the diagonal phase-shift matrix of the RIS can be represented by Φ, where $\Phi = diag(\theta) = \mathbf{diag}(\mathbf{e^{j\phi_1}}, \mathbf{e^{j\phi_2}}, ..., \mathbf{e^{j\phi_N}})$. The channel from the BS to the UE through the RIS can be modeled as a cascaded channel H_c, considering the RIS reflection with controllable phase shifts, that can be defined as $H_c = \mathbf{h}^T \Phi \mathbf{g}$. The channel gains from the BS to element n in the RIS structure, and between element n and the UE can be expressed, respectively, as follows

$$h_n = r_n^{-\delta/2} \alpha_n e^{-j\varphi_n}, \quad g_n = l_n^{-\delta/2} \beta_n e^{-j\psi_n} \tag{1}$$

where r and l represent the distances for the links between the BS and RIS and between the RIS and UE, respectively (assuming that $r_n \approx r$, and $l_n \approx l$, $\forall n = [1, 2, ..., N]$ due to the limited dimensions of the RIS and UE), δ is the path-loss exponent, φ_n and ψ_n are the channel gains' phases, and α_n and β_n are their amplitudes that follow Nakagami-m distribution with shape parameter m_i and scale parameter Ω_i, with $i \in \{1, 2\}$ for the first and second hops, respectively. The probability distribution of the amplitude of the channel gain w, where $w \in \{\alpha, \beta\}$, is described by the Nakagami-m fading distribution and can be expressed as follows [13]:

$$f_w(x) = \frac{2m^m x^{2m-1}}{\Omega^m \Gamma(m)} exp(\frac{-mx^2}{\Omega}) \tag{2}$$

Authorized licensed use limited to: Queen's University. Downloaded on August 21,2024 at 11:21:21 UTC from IEEE Xplore. Restrictions apply.

where $\Gamma(.)$ is the gamma function.

In our analysis, we will focus on a far-field scenario, where the distance from the BS/UE to the RIS is greater than $\frac{2D^2}{\lambda}$, with λ being the wavelength and D as the largest dimension of the RIS [14]. Furthermore, we assume that the RIS has complete information about the phases of the channels in h_n and $g_n, \forall n = [1, 2, ..., N]$. Then, the phase shifts $\phi = [\phi_1, ..., \phi_N]$ are adjusted to eliminate the channel phases and maximize the SNR at the UE as in [15], by setting $\phi_n = \varphi_n + \psi_n$ for $n = 1, 2, ..., N$. Thus, the amplitude of the cascaded channel gain can be represented as

$$\begin{aligned} |H_c| &= |h|^T |g| = \sum_{n=1}^{N} |h_n||g_n| \\ &= r^{-\delta/2} l^{-\delta/2} \sum_{n=1}^{N} \alpha_n \beta_n \end{aligned} \tag{3}$$

Accordingly, the received SNR by the UE can be modeled as

$$\gamma = \frac{P|H_c|^2}{N_0} = \frac{P}{N_0}\ r^{-\delta} l^{-\delta}\ (\sum_{n=1}^{N} \alpha_n \beta_n)^2 \tag{4}$$

where P is the BS's downlink transmit power, and N_0 represents the variance of the additive white Gaussian noise (AWGN) at the UE receiver.

III. Delay Analysis Over RIS-Assisted link

The average packet delay includes the packet transmissions and retransmissions, as well as the queuing delay on the cascaded link. Additionally, the analysis employs an adaptive M-QAM modulation model that adjusts the modulation order in response to the channel state.

A. Channel Modeling

From (3), the channel of the signal when passing through element n has an amplitude that is modeled by scaled double Nakagami-m distribution and can be represented as $Z_n = \alpha_n \beta_n$ and scaled with $\xi(r, l) = r^{-\delta/2} l^{-\delta/2}$. Therefore, the amplitude of the overall cascaded channel gain can be expressed as $|H_c| = \xi(r, l) \sum_{n=1}^{N} Z_n$, where the constituent variables of Z_n, i.e., α_n and β_n, being independent but not necessarily identically distributed.

When a large number of reflecting elements N are deployed in the RIS, the central limit theorem (CLT) is applicable. This means that the summation $\sum_{n=1}^{N} Z_n$ follows a normal distribution and is scaled by $\xi(r, l)$. Consequently, the probability density function (PDF) of $|H_c|$ approaches the Gaussian distribution with a mean of μ and variance of σ^2, as follows

$$\begin{aligned} |H_c| &\sim \mathcal{N}(\mu, \sigma^2) \\ \mu = \xi(r, l) N \mathbb{E}[Z_n], &\quad \sigma^2 = \xi(r, l)^2 N var(Z_n) \end{aligned} \tag{5}$$

The mean of Z_n and its variance can be calculated as follows [13]

$$\begin{aligned} \mu_Z = \mathbb{E}[Z_n] &\triangleq \prod_{i=1}^{2} \frac{\Gamma(m_i + 1/2)}{\Gamma(m_i)} (\frac{\Omega_i}{m_i})^{1/2}, \\ \sigma_Z^2 = var(Z_n) &\triangleq \mathbb{E}[Z_n^2] - \mathbb{E}[Z_n]^2 \\ = \prod_{i=1}^{2} \frac{\Gamma(m_i + 1)}{\Gamma(m_i)} (\frac{\Omega_i}{m_i}) &- (\prod_{i=1}^{2} \frac{\Gamma(m_i + 1/2)}{\Gamma(m_i)} (\frac{\Omega_i}{m_i})^{1/2})^2 \end{aligned} \tag{6}$$

Consequently, the PDF of $|H_c|^2$ can be expressed as a non-central chi-square distribution with one degree of freedom, which is defined as [16]

$$f_{|H_c|^2}(x) = \frac{1}{2\sigma^2}\ (\frac{x}{\lambda_c})^{-\frac{1}{4}}\ exp(-\frac{x + \lambda_c}{2\sigma^2})\ I_{-\frac{1}{2}}(\frac{\sqrt{x\lambda_c}}{\sigma^2}) \tag{7}$$

where $I_\upsilon(z)$ denotes the modified Bessel function of the first class with order υ, and $\lambda_c = \mu^2 = (\xi(r, l) N \mathbb{E}[Z_n])^2$. According to (4), the PDF of the SNR, γ, can be represented as

$$f_\gamma(\gamma) = \frac{1}{2\sigma^2 \overline{\gamma}}\ (\frac{\gamma}{\overline{\gamma}\lambda_c})^{-\frac{1}{4}}\ exp(-\frac{\gamma + \lambda_c \overline{\gamma}}{2\overline{\gamma}\sigma^2})\ I_{-\frac{1}{2}}(\frac{\sqrt{\gamma\lambda_c}}{\sqrt{\overline{\gamma}\sigma^2}}) \tag{8}$$

where $\overline{\gamma} = P/N_0$ denotes the average SNR.

Using (8), the cumulative distribution function (CDF) of γ can be given as follows

$$F_\gamma(\gamma) = 1 - Q_{\frac{1}{2}}(\frac{\sqrt{\lambda_c}}{\sigma}, \frac{\sqrt{\gamma}}{\sqrt{\overline{\gamma}}\sigma}) \tag{9}$$

where Q_ι(a,b) is the Marcum Q-function and defined in [17].

B. Average Packet Delay

Determining the average transmission delay of a packet involves dividing the SNR range into L regions based on the specified distribution. A constellation with a size of M_ℓ, where $M_\ell = 2^\ell$ and (ℓ= 1,2,3,…,L), is utilized in each region. Moreover, the determination of the SNR boundaries for the various regions, which can be denoted by $\vartheta_1, \vartheta_2, \vartheta_3, ..., \vartheta_L$ where $\vartheta_1 < \vartheta_2 < \vartheta_3 < ... < \vartheta_L$, is carried out to ensure that the BER remains below a certain threshold value (BER_{th}). Hence, the scheme adjusts the modulation order based on the link's SNR to meet the target (BER_{th}). Specifically, the regions' boundaries can be calculated as follows [18]

$$\vartheta_\ell = \begin{cases} [erfc^{-1}(2BER_{th})]^2, & \ell = 1. \\ \frac{2}{3} K_0 (2^\ell - 1), & \ell = 2, 3, ...L. \end{cases} \tag{10}$$

where $erfc^{-1}()$ is the inverse complementary error function, and $K_0 = -\ln(5BER_{th})$. The model assumes time-slotted transmission, where each time slot has a duration of τ. Then, the expression for the number of bits that can be sent within a time slot duration is given by the following

$$b_\ell = \tau\ B\ \log_2(1 + \vartheta_\ell) \tag{11}$$

where B is the link's bandwidth.

Therefore, if a packet of size Q bits is needed to be transmitted, the number of time slots required to deliver this

Authorized licensed use limited to: Queen's University. Downloaded on August 21,2024 at 11:21:21 UTC from IEEE Xplore. Restrictions apply.

packet is $\epsilon_\ell = \lceil Q/b_\ell \rceil$. As a result, if the packet is being transmitted while the SNR over the channel is in the region $[\vartheta_\ell, \vartheta_{\ell+1}]$ and the modulation order is M_ℓ, the time required to transmit the packet is determined as follows

$$t_\ell = \epsilon_\ell \ \tau = \lceil \frac{Q}{b_\ell} \rceil \ \tau \tag{12}$$

According to the SNR distribution in (8) and (9) for the RIS-assisted link, the average transmission delay over that link can be determined as

$$\begin{aligned} D_t = \varkappa_r t_1 Pr(\gamma < \vartheta_1) + \sum_{\ell=1}^{L-1} t_\ell Pr(\vartheta_\ell \leqslant \gamma < \vartheta_{\ell+1}) \\ + t_L Pr(\gamma \geqslant \vartheta_L) \end{aligned} \tag{13}$$

The first term in (13) represents the mean time to transmit the packet if the SNR falls below the minimum boundary value (ϑ_1), where a packet retransmission is needed and thus, causing an extra delay. The average number of transmissions needed to achieve successful delivery of a packet is represented by the term $\varkappa_r$. $\varkappa_r$ can be obtained as $\varkappa_r = \frac{1}{P_s}$, where P_s denotes the probability of successful transmission which can be determined using the distribution in (9). Similarly, the probabilities of the remaining regions in (13) can be calculated by utilizing the CDF of the SNR distribution mentioned in (9).

We obtain the queuing delay on the RIS-assisted link, which refers to the time a packet spends waiting in a queue before being transmitted, using an M/G/1 queuing model, as the analysis employs adaptive modulation that makes the service time dependent on the channel's state. Then, the expectation of the packet's waiting time can be expressed as

$$\mathbb{E}[D_w] = \mathbb{E}[q] \ D_t + \mathbb{E}[R_q] \tag{14}$$

where $\mathbb{E}[q]$ refers to the average number of packets waiting in the queue, while R_q is the amount of time remaining for the packets being processed. Subsequently, it is possible to represent the average queue length $\mathbb{E}[q]$ in terms of the average waiting time, by utilizing Little's theorem, as $\mathbb{E}[q] = \lambda_p \ \mathbb{E}[D_w]$, where the arrival rate in packets per second is denoted by λ_p, then the average waiting time can be represented by

$$\mathbb{E}[D_w] = \frac{\mathbb{E}[R_q]}{1 - \rho_p} \tag{15}$$

where $\rho_p = \lambda_p \ D_t$. Consequently, by utilizing the Pollaczek-Khinchin formula, it is possible to express the average waiting time of a packet as follows

$$\mathbb{E}[D_w] = \frac{1 + C^2}{2} \frac{\rho_p}{1 - \rho_p} D_t \tag{16}$$

Here, C^2 is the squared coefficient of variation and can be determined as $C^2 = \sigma_p^2 / D_t^2$, where σ_p^2 denotes the variance of the packet's service time and can be expressed as

$$\begin{aligned} \sigma_p^2 = (\varkappa_r t_1 - D_t)^2 \ Pr(\gamma < \vartheta_1) \\ + \sum_{\ell=1}^{L-1} (t_\ell - D_t)^2 \ Pr(\vartheta_\ell \leqslant \gamma < \vartheta_{\ell+1}) \\ + (t_L - D_t)^2 \ Pr(\gamma \geqslant \vartheta_L) \end{aligned} \tag{17}$$

Finally, the total average packet delay, which consists of the transmission and queuing delays, can be determined by $D_p^{tot} = D_t + \mathbb{E}[D_w]$.

IV. Performance Evaluation

In this section, we present the effect of different performance metrics on the average packet delay, which encompasses both transmission and queuing delays over the RIS-assisted link. The packet delay performance is influenced by several factors, such as the average SNR across the link, the number of passive reflecting elements in the RIS, and the transmission distances. We also consider the impact of different Nakagami fading parameters. The downlink bandwidth allocated to the BS is B = 100 MHz. Furthermore, unless stated otherwise, the distances for the RIS-assisted link are $r = 60m$, $l = 30m$, and the path loss exponent is set as $\delta = 2.2$. We consider six distinct regions, L=6, within the SNR range. Each region has a designated modulation order and is determined by certain boundary values dependent on the target BER. Moreover, we use a threshold BER of 10^{-5} and a packet size of 1500 bytes. To verify our analysis, we perform Monte Carlo (MC) simulations involving 10^5 iterations.

Fig. 2 shows the effect of the link's average SNR on the average delay for successful packet transmission. We can observe that the mean packet delay decreases with the increase in the link's quality and average SNR. Moreover, increasing the number of elements N in the RIS significantly improves the delay performance. As observed, some ranges of the SNR have approximately the same average delay. The reason is that the number of time slots required to transmit the packet is equal in some contiguous SNR regions as a result of taking the ceiling function in (12). As a result, increasing the average SNR within these regions will only change the probability of such SNR regions that have the same delay in (13). In contrast, other regions have a very low probability, rendering the average packet delay approximately constant. Then, in the decreasing part, after the curve knee, changing the average SNR will change the probability of regions that have different transmission delays, i.e., increasing the average SNR will increase the probability of the higher SNR region with a lower transmission delay due to the higher modulation order, thus, decreasing the average packet delay. Fig. 3 shows how the fading conditions when $N = 200$ influence the delay performance. As m_1 and m_2 increase, with increasing the average SNR, the delay decreases at lower SNR values due to the decrease in fading severity. Note that, at high average SNR, the probability of being in the higher SNR region with higher modulation order is dominant. Fig. 4 illustrates the impact of the distance separating the UE and RIS on the average delay. It is apparent from the figure that as the distance of the UE-RIS link increases, there is a corresponding increase in the average packet delay. Furthermore, as previously explained, some regions on the curve exhibit nearly constant delays due to the use of the ceiling function for time slot calculations. This results in the same transmission delay for contiguous SNR regions, e.g., $t_5 = t_6$. Consequently, variations in

Authorized licensed use limited to: Queen's University. Downloaded on August 21,2024 at 11:21:21 UTC from IEEE Xplore. Restrictions apply.

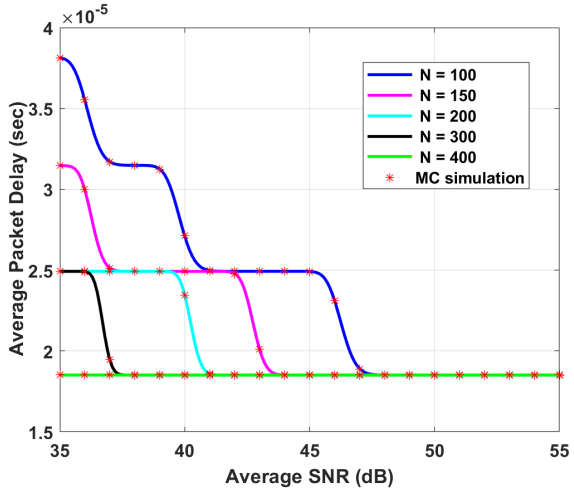

Fig. 2. The relationship between the average packet delay and the average SNR when $\delta = 2.2$, and $m_1 = m_2 = 2$, $r = 60m$, and $l = 30m$ in the RIS-assisted link.

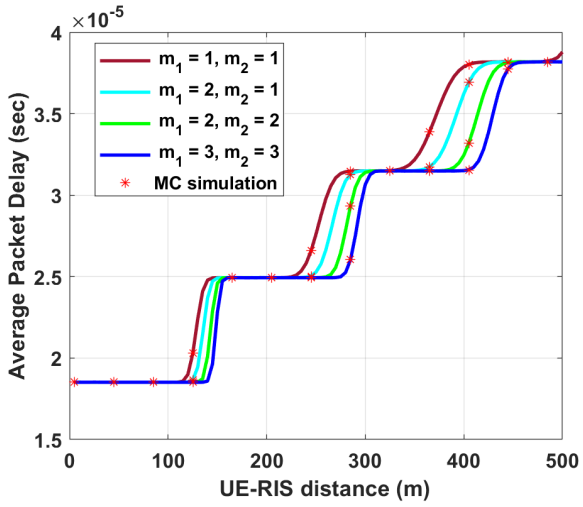

Fig. 4. Average packet delay versus the UE-RIS distance when $\delta = 2.2$, $N = 250$, and $r = 50m$ in the RIS-assisted link.

distance within these regions primarily affect the probabilities of these contiguous SNR regions, resulting in the same average delay with slight changes. This is because other regions with very low probabilities have a minimal impact on the average delay. At lower distances in Fig. 4, higher probabilities are given to the SNR regions characterized by higher modulation orders, resulting in a low average packet delay. Extending the transmission distance increases the average packet delay due to the increased probability of the SNR regions with lower modulation orders and longer delays. Moreover, the delay performance enhancement can be observed by increasing the fading shape parameters m_1 and m_2, which provides a longer UE-RIS distance before the delay degradation. The average packet delay experienced by the typical UE is depicted in Fig. 5 concerning the distance from the RIS, and the number of RIS reflecting elements N. It is evident that as the distance

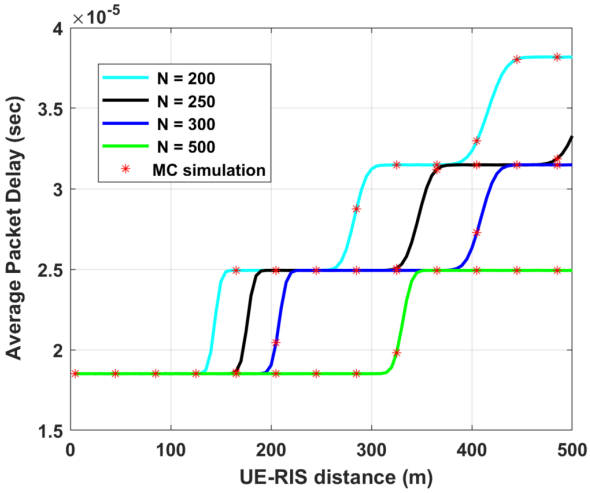

Fig. 5. Average packet delay versus the UE-RIS distance when $\delta = 2.2$, $m_1 = m_2 = 2$, and $r = 50m$.

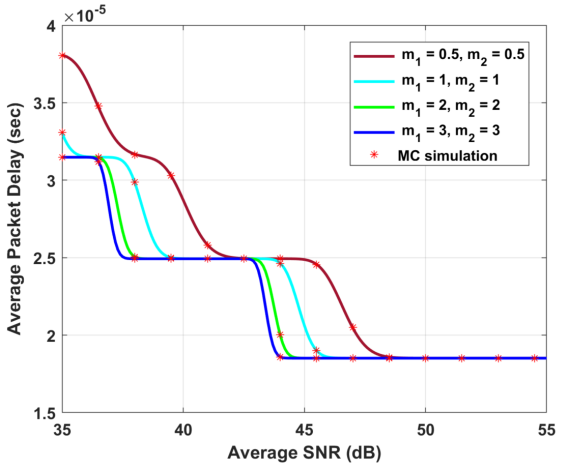

Fig. 3. Average packet delay variation with the average SNR when $\delta = 2.2$, $N = 200$, $r = 60m$, and $l = 30m$ in the RIS-assisted link.

between the RIS and UE increases and the number of RIS elements decreases, the average packet delay of the typical UE rises more quickly compared to scenarios with a larger number of RIS elements. Fig. 6 shows how the delay performance is affected by increasing the number of passive reflecting elements, N. The average packet delay decreases significantly with increasing N. Moreover, mitigating the severity of fading (i.e., increasing the shape parameter m) helps to improve the delay performance as the average delay will be better for the same number of reflecting elements N. Fig. 7 also illustrates that the received SNR at the UE can be substantially improved by increasing the number of reflecting elements in the RIS and, thus, reducing the average packet delay. Furthermore, an increase in the average packet delay experienced by the UE can be observed when the UE-RIS distance is expanded.

Authorized licensed use limited to: Queen's University. Downloaded on August 21,2024 at 11:21:21 UTC from IEEE Xplore. Restrictions apply.

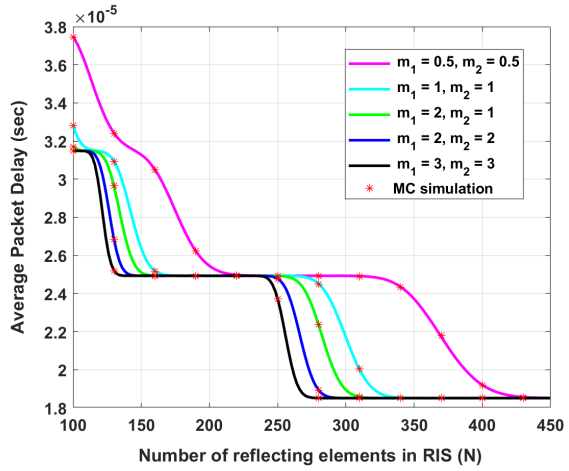

Fig. 6. Average packet delay variation with the number of passive reflecting elements N when $\delta = 2.4$, $r = 60m$, and $l = 60m$.

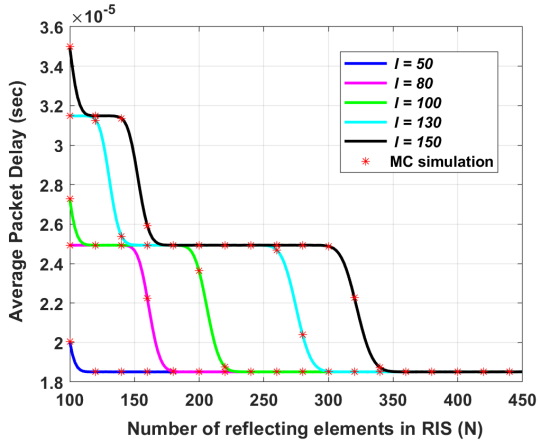

Fig. 7. Average packet delay versus the number of passive reflecting elements N when $\delta = 2.2$, $m_1 = m_2 = 2$, and $r = 60m$.

From the described figures, it is evident that the analytical curves closely match those obtained from Monte Carlo simulations. This strong agreement validates the accuracy of the derived expressions.

V. Conclusion

This paper examines the delay performance of the RIS-assisted link under Nakagami-m channels. We analyze transmission and queuing delays based on the SNR distribution and channel conditions. We study the impact of various parameters on the average delay performance, including the number of reflecting elements, average SNR, and distance between the user and RIS. Our findings show that increasing the number of reflecting elements in the RIS can significantly improve the received signal at the user and leads to better average packet delay. Additionally, our results demonstrate how packet delay can be greatly enhanced when fading conditions are not severe. In future work, we will explore a more general setup with multi-RIS architecture and analyze the packet delay over multi-hop links. Moreover, the outcomes of this paper can be exploited in multi-user scenarios, where the packet delay serves as a key metric in tackling the user-RIS association problem based on the delay requirements of the user.

References

[1] Q. Wu, S. Zhang, B. Zheng, C. You, and R. Zhang, "Intelligent Reflecting Surface-Aided Wireless Communications: A Tutorial," *IEEE Transactions on Communications*, vol. 69, no. 5, pp. 3313–3351, 2021.

[2] M. H. Samuh, A. M. Salhab, and A. H. A. El-Malek, "Performance Analysis and Optimization of RIS-Assisted Networks in Nakagami-m Environment," *02 August 2021, PREPRINT (Version 1) available at Research Square [https://doi.org/10.21203/rs.3.rs-706423/v1].*

[3] A.-A. A. Boulogeorgos and A. Alexiou, "Performance Analysis of Reconfigurable Intelligent Surface-Assisted Wireless Systems and Comparison With Relaying," *IEEE Access*, vol. 8, pp. 94 463–94 483, 2020.

[4] D. Tyrovolas, S. A. Tegos, E. C. Dimitriadou-Panidou, P. D. Diamantoulakis, C. K. Liaskos, and G. K. Karagiannidis, "Performance Analysis of Cascaded Reconfigurable Intelligent Surface Networks," *IEEE Wireless Communications Letters*, vol. 11, no. 9, pp. 1855–1859, 2022.

[5] P. Yang, L. Yang, and S. Wang, "Performance Analysis for RIS-Aided Wireless Systems With Imperfect CSI," *IEEE Wireless Communications Letters*, vol. 11, no. 3, pp. 588–592, 2022.

[6] T. Bao, H. Wang, H.-C. Yang, W.-J. Wang, and M. O. Hasna, "Performance Analysis of RIS-aided Communication Systems over the Sum of Cascaded Rician Fading with imperfect CSI," in *IEEE Wireless Communications and Networking Conference (WCNC)*, 2022, pp. 399–404.

[7] L. Yang, P. Li, Y. Yang, S. Li, I. Trigui, and R. Ma, "Performance Analysis of RIS-Aided Networks With Co-Channel Interference," *IEEE Communications Letters*, vol. 26, no. 1, pp. 49–53, 2022.

[8] D. Do, A. Le, and S. Mumtaz, "Secure Performance Analysis of RIS-aided Wireless Communication Systems," in *IEEE Global Communications Conference (GLOBECOM)*, 2021, pp. 01–06.

[9] D. Selimis, K. P. Peppas, G. C. Alexandropoulos, and F. I. Lazarakis, "On the Performance Analysis of RIS-Empowered Communications Over Nakagami-m Fading," *IEEE Communications Letters*, vol. 25, no. 7, pp. 2191–2195, 2021.

[10] Z. Liu, X. Yue, C. Zhang, Y. Liu, Y. Yao, Y. Wang, and Z. Ding, "Performance Analysis of Reconfigurable Intelligent Surface Assisted Two-Way NOMA Networks," *IEEE Transactions on Vehicular Technology*, vol. 71, no. 12, pp. 13 091–13 104, 2022.

[11] Y. Zhang, J. Zhang, M. D. Renzo, H. Xiao, and B. Ai, "Performance Analysis of RIS-Aided Systems With Practical Phase Shift and Amplitude Response," *IEEE Transactions on Vehicular Technology*, vol. 70, no. 5, pp. 4501–4511, 2021.

[12] N. Moosavi, A. Zappone, P. Azmi, and M. Sinaie, "Delay-Aware and Energy-Efficient Resource Allocation for Reconfigurable Intelligent Surfaces," *IEEE Communications Letters*, vol. 27, no. 2, pp. 605–609, 2023.

[13] G. K. Karagiannidis, N. C. Sagias, and P. T. Mathiopoulos, "$N*$Nakagami: A Novel Stochastic Model for Cascaded Fading Channels," *IEEE Transactions on Communications*, vol. 55, no. 8, pp. 1453–1458, 2007.

[14] W. Tang, M. Z. Chen, X. Chen, J. Y. Dai, Y. Han, M. Di Renzo, Y. Zeng, S. Jin, Q. Cheng, and T. J. Cui, "Wireless Communications With Reconfigurable Intelligent Surface: Path Loss Modeling and Experimental Measurement," *IEEE Transactions on Wireless Communications*, vol. 20, no. 1, pp. 421–439, 2021.

[15] Q. Wu and R. Zhang, "Intelligent Reflecting Surface Enhanced Wireless Network via Joint Active and Passive Beamforming," *IEEE Transactions on Wireless Communications*, vol. 18, no. 11, pp. 5394–5409, 2019.

[16] J. G. Proakis and M. Salehi, *Digital Communications*. McGraw-hill New York, 2001, vol. 4.

[17] V. M. Kapinas, S. K. Mihos, and G. K. Karagiannidis, "On the Monotonicity of the Generalized Marcum and Nuttall Q -Functions," *IEEE Trans. on Inf. Theory*, vol. 55, no. 8, pp. 3701–3710, 2009.

[18] M.-S. Alouini and A. J. Goldsmith, "Adaptive Modulation Over Nakagami Fading Channels," *Wireless Personal Communications*, vol. 13, pp. 119–143, 2000.

Authorized licensed use limited to: Queen's University. Downloaded on August 21,2024 at 11:21:21 UTC from IEEE Xplore. Restrictions apply.